11-4-2010

X-RHex: A Highly Mobile Hexapedal Robot for Sensorimotor Tasks

Kevin C. Galloway
University of Pennsylvania, kcgalloway@gmail.com

Galen Clark Haynes
University of Pennsylvania, gchaynes@seas.upenn.edu

B. Deniz Ilhan
University of Pennsylvania, bdeniz@seas.upenn.edu

Aaron M. Johnson
University of Pennsylvania, aaronjoh@seas.upenn.edu

Ryan Knopf
University of Pennsylvania, rknopf@seas.upenn.edu

See next page for additional authors

Author(s)
Kevin C. Galloway, Galen Clark Haynes, B. Deniz Ilhan, Aaron M. Johnson, Ryan Knopf, Goran A. Lynch, Benjamin N. Plotnick, Mackenzie White, and Daniel E. Koditschek

X-RHex: A Highly Mobile Hexapedal Robot for Sensorimotor Tasks

Kevin C. Galloway* G. C. Haynes† B. Deniz Ilhan†
Aaron M. Johnson† Ryan Knopf* Goran Lynch†
Benjamin Plotnick† Mackenzie White† D. E. Koditschek†

November 4, 2010

Abstract

We report on the design and development of *X-RHex*, a hexapedal robot with a single actuator per leg, intended for real-world mobile applications. X-RHex is an updated version of the RHex platform, designed to offer substantial improvements in power, run-time, payload size, durability, and terrain negotiation, with a smaller physical volume and a comparable footprint and weight. Furthermore, X-RHex is designed to be easier to build and maintain by using a variety of commercial off-the-shelf (COTS) components for a majority of its internals. This document describes the X-RHex architecture and design, with a particular focus on the new ability of this robot to carry modular payloads as a *laboratory on legs*. X-RHex supports a variety of sensor suites on a small, mobile robotic platform intended for broad, general use in research, defense, and search and rescue applications. Comparisons with previous RHex platforms are presented throughout, with preliminary tests indicating that the locomotive capabilities of X-RHex can meet or exceed the previous platforms. With the additional payload capabilities of X-RHex, we claim it to be the first robot of its size to carry a fully programmable GPU for fast, parallel sensor processing.

1 Introduction

Despite the images of agile humanoid or animal-like robots long held in the public imagination, legged robots capable of dynamic locomotion have only recently been developed. One of the first such dynamical machines is RHex [1], a hexapod with a single, unrestricted rotary actuator per leg. While mechanically simple, this design has achieved a variety of interesting locomotion tasks, including walking, running [1], pronking [2, 3], leaping and flipping [4], climbing stairs [5], and even running upright on its rear legs [6]. A number of robots have been built based on the RHex concept. Prior platforms include: Research RHex [1], the product of the original DARPA-funded consortium; Rugged RHex [7, 8, 9], a hardened, commercialized version built by Boston Dynamics, Inc.; EduBot [10], a machine developed at the University of Pennsylvania for use in a classroom setting; AQUA [11], an amphibious robot

*Mechanical Engineering and Applied Mechanics, University of Pennsylvania, 220 S. 33rd St., Philadelphia, PA 19104

†Electrical and Systems Engineering, University of Pennsylvania, 200 S. 33rd St., Philadelphia, PA 19104

with paddles instead of legs; SensoRHex [12], a recent update to the RHex design focusing on modularity and sensor integration developed at Bilkent University; as well as a host of more minor platform revisions spanning a decade's research efforts. In this paper, we describe the development and implementation of the newest descendant in the line of RHex robots, X-RHex.

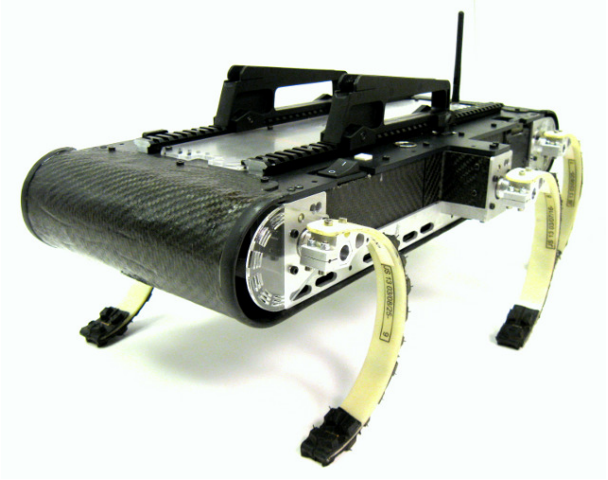

Figure 1: The X-RHex robot with handles attached.

The new design represents a thorough and substantial update of the Research RHex platform and incorporates a number of technologies unavailable at the point of introduction of the first RHex platform a decade ago. In particular, we have relied heavily on previously unavailable commercial-off-the-shelf (COTS) components, resulting in a robot that matches the footprint of the original Research RHex machine with approximately half the volume and considerably simplified fabrication and maintenance. Moreover, X-RHex boasts a number of substantial improvements in the capabilities of its mechanical and electrical systems which make it capable of both highly dynamic maneuvers and sensor-rich autonomous behaviors.

One major contribution of the new platform, and a design extension beyond prior RHex platforms, is the introduction of a payload system on the top of the robot. The system consists of a standardized mechanical mount and a set of electrical connectors to interface the payloads with on-board electronics. With swappable payloads, the robot functions as a *laboratory on legs* and supports an open-ended variety of experiment-specific sensory and computational payloads. In particular, X-RHex is the first robot of its size to support a payload computer that includes a multi-core programmable GPU.

This report documents the design decisions and architectural choices of the X-RHex robot, including descriptions of the mechanical, electrical, and software improvements over past RHex platforms. Preliminary behavioral results are presented as a basis of comparison to other RHex-like robots. In addition, we detail the new modular payload system and suggest real-world applications for the robot. New behaviors, further experimental results, and added capabilities will be presented in future work.

The rest of this paper is organized as follows:

- Section 2 provides an overview of the design of X-RHex, detailing the robot's mechanical design, motor selection, electronic components, and software.

- Section 3 describes the payload system and envisioned applications for this new robot.
- Section 4 provides initial comparisons between X-RHex and prior RHex platforms.
- Section 5 gives some concluding thoughts and possible directions for future work.

2 Robot Description

X-RHex's design differs substantially from those of its predecessors. The robot's body is compact and thin in profile, with physical strength greatly exceeding that of Research RHex (see Section 4 for a more detailed comparison). Our team's experience with the RiSE V3 platform [13] led us to choose high power density brushless DC motors, and drive those motors using COTS motor controllers. Communications between the main computer and motor control modules operate over USB, while the robot's control software uses a new real-time robotics package called *Dynamism*[1]. The robot's mechanical structure is described in Section 2.1, motor technology in Section 2.2, electronics in Section 2.3, and software in Section 2.4.

2.1 Mechanical Design

The main objectives for the mechanical design of X-RHex were to improve frame durability (both in resistance to fatigue and impact) and overall robot serviceability while achieving similar or better performance to past robots. The overall dimensions (57x39x7.5 cm) were intended to maintain as much similarity to Research RHex (54x39x13.9 cm) as possible. The most notable difference is that the X-RHex frame is much shorter at a total height of 7.5cm. Lateral inter-leg distances are identical, but longitudinal inter-leg distances are 2cm greater. Research RHex leg design [14, 5] was preserved, and since the leg mounts are nearly centered on an overall thinner body, the robot can operate with greater ground clearance even when in an inverted state. This is a useful feature in the eventuality of robot inversion in a constrained space [4].

2.1.1 Body Design

The X-RHex frame is light and stiff to optimize locomotive performance, and sufficiently strong to protect hardware and maintain structural integrity even when subjected to severe impacts. The body features a bottom frame and a top plate, as seen in Figure 2a. The bottom frame is constructed from several aluminum 7075-T6 structural pieces including two runners and three cross pieces. The top plate is made from a single sheet of 1/8" aluminum. The alloy Al-7075 was selected for its high yield strength and machinability [15]. Though a monolithic base was considered, a multi-component base frame is more serviceable (i.e. for repairing damaged sections) and adaptable to future design iterations.

The motor mount assemblies are anchored at the ends of each cross piece and function as structural elements connecting the bottom and top frames (see Figure 2), and are discussed further in Section 2.1.2. This configuration increases the overall structural stiffness of the frame by increasing the second moment of inertia with a minimal increase in frame mass [16].

[1] Dynamism, http://www.dynamism-project.com/

Two non-structural cross pieces in the bottom frame act as heat sinks for the motor controllers (see Figure 2b). This arrangement was chosen for two reasons: 1) to consolidate three motor controllers into a single, easily removable, electronics module (see Section 2.3.2), and 2) to provide a larger thermal mass for the motor controllers to sink heat into.

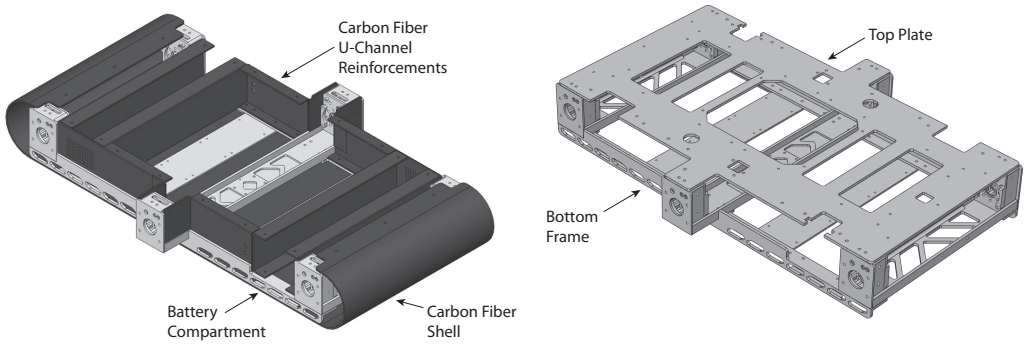

(a) The full frame with internal components removed.

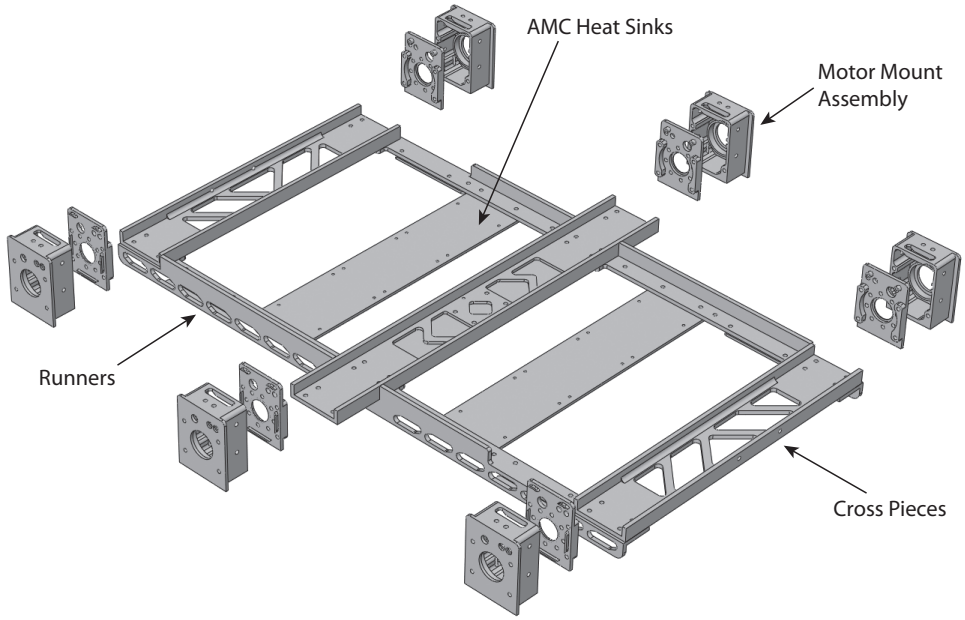

(b) Exploded view of aluminum frame components without top plate or composite pieces.

Figure 2: Mechanical construction of the robot.

Carbon fiber panels, as seen in Figure 2a, were added to increase frame stiffness and to protect the robot from outside obstacles while not significantly increasing body weight. Specifically, carbon fiber U-channels line the sides and serve the dual purpose of reinforcing the frame and enclosing internal components. A carbon fiber shell slides on from the side of the robot to provide additional protection to the front, back, and bottom of the robot.

Two rectangular carbon fiber battery compartments are positioned symmetrically in the

front and rear of the robot; their locations were chosen such that the center of mass is conserved (see Figure 2a). The batteries themselves are held in non-conductive fiberglass cases equipped with spring-loaded latches to enable quick and tool-less battery swapping.

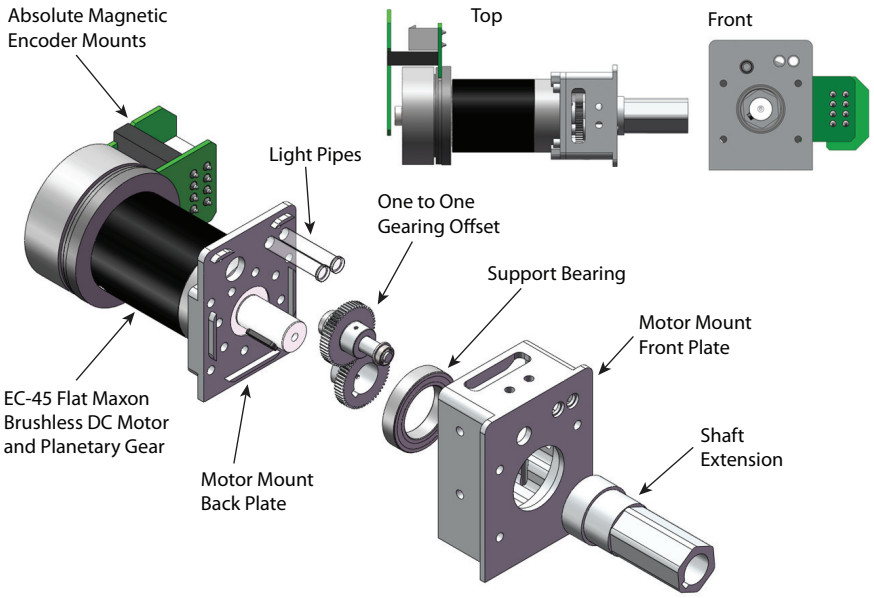

Figure 3: Exploded view of the motor mounting assembly (leg and leg mount not included).

2.1.2 Motor Mount Assembly

The motor mount assembly offers two enhancements over Research RHex. First, it acts as a support member to stiffen the frame by rigidly connecting the bottom frame to the top plate. Second, it now includes accurate estimation of absolute leg position. This estimation is achieved by an offset secondary shaft which rotates with the main motor shaft using adjacent spur gears of equal size (see Figure 3). The secondary shaft is monitored by an absolute encoder to provide a measurement of absolute leg position. With this measurement the need for any calibration routine on startup is eliminated.

After the spur gear is an aluminum shaft extension, as seen in Figure 3. In Research RHex, shaft extensions were added to the motor shaft and supported by a bearing to 1) reduce transverse loads to the motor shaft and gear box and 2) to extend the reach of the motor shaft for leg attachment. These extensions were manufactured using wire EDM [17] to match the inner wall of the extension to the profile of the motor shaft, and were permanently epoxied together. The X-RHex shaft extensions were milled using conventional machining practices and are not epoxied to the motor, which allows the shaft extension and motor mount to be separated from the motor for maintenance or replacement if needed. The motor shaft features a 3mm wide by 8 mm long key which mates with a slotted feature on the shaft extension. The shaft extension necks down before extending through the support bearing on the motor

mount assembly thus preventing the shaft extension from sliding out and securing the support bearing in place.

At the end of the shaft extension is a leg mount that connects to the fiberglass C-legs. Research RHex leg mounts offer a coupled solution where the same screws that attach the C-legs to the mount also anchor the mount to the shaft extension [5]. The X-RHex design decouples these two such that the C-leg can be removed without removing the leg mount and vice versa.

2.2 Motor Selection

Motor sizing for RHex-like robots poses challenges distinct from those offered by most other motor-sizing tasks (covered well in [18]). First and foremost, the motor/gearbox combination must operate over an unusually wide range of operational speeds[2]. X-RHex is intended to perform slow speed activities requiring large leg torques, such as clambering over rocks and climbing stairs, as well as high speed activities with moderate torques, like running at high speeds or walking with high duty-factor gaits. There are few non-robotics applications in which a motor operates at both its stall torque and its no-load speed within a short period of time. Our most reliable understanding of a RHex-like machine's motor operating regime comes from Research RHex data. While our ongoing research entails the development of simulation and analytical tools for motor sizing in robotic applications [21], we were able to choose motors for X-RHex based on empirical data from Research RHex.

Our first significant design decision was to support brushless motors. The principal downside to brushless technology is the complexity of controlling these motors [22]. The commercial motor controller boards described in Section 2.3.2, however, manage most aspects of brushless motor commutation and control, and provide an extensive API, trading the cost of design effort and hardware complexity for the effort of learning how to effectively use the manufacturer's motor control interface. While the efficiency and service life benefits of brushless motors are often touted [22], the primary advantage, for our application, is the option to use high-torque, flat "pancake-style" brushless motors offered by Maxon Motors[3]. Inverting the design of most "pencil" motors, these pancake motors consist of an internal stator containing the windings, surrounded by a rotor containing a permanent magnet ring. The rotor is part of the back of the motor and is exposed while spinning. Because of the large rotor diameter, the motors are very short and light (110g, less than half the mass of an equivalently powerful pencil motor), though with a slower mechanical time constant due to the increased rotor inertia. The small footprint and tiny mass of these motors is overwhelmingly appealing in a mobile robotics application, and, following team experience with RiSE V3 [13], provided us with perhaps the strongest incentive to support brushless technology.

Within the pancake form factor, there are a number of motor options. We limited our choice to those nominally specified to deliver 50W, exceeding the Research RHex motor power specification (20W) by more than a factor of 2. In the computation of motor parameters, care was taken on a number of points: first, given parameters for each motor were compensated based on our battery voltage, as each motor is specified relative to a given nominal voltage, while X-RHex's electrical system was designed around a 37V battery (this choice is discussed

[2]Research RHex has demonstrated near-stall operation during leaping tasks [19], and exhibited leg speeds very near no-load during high-speed running [20].

[3]Maxon provides a collection of motors in finely grained size and power increments; we have not encountered other manufacturers with similarly comprehensive options at the scales and quality of interest to us.

in Section 2.3.4). Therefore, we recompute relevant motor parameters using a voltage of 37V, using the standard linear motor model as presented in [23]. Using a voltage different from the nominal voltage specified by Maxon in their product line documentation affects the computation of a motor's apparent stall torque and no-load speed, though not the motor's maximum continuous torque, which is governed purely by the thermal influence of current running through the motor. Second, our motor controllers limit peak instantaneous motor current to 20A. However, with the 37V supply on X-RHex, some motors are capable of drawing more than 20A at low speeds. Thus, we also denote an "Achievable Stall Torque," the torque that corresponds to the controller's maximum current output. Our chosen motor dramatically exceeds the Research RHex motor in its achievable stall torque (670mNm vs 257mNm) and maximum continuous torque (83.1mNm vs 26.7mNm), though it has a slightly lower no-load speed (10314rpm vs 13600rpm). In principle, the X-RHex motor is capable of much higher power output than its predecessor. However, motor thermal constraints pose real operational limitations and are harder to assess without a specification of the target task domain. We discuss thermal behavior in greater detail in Section 2.2.1. The parameters for our chosen motor are shown next to those of Research RHex in Table 1.

Attribute	Research RHex Motor	X-RHex Motor
Type	Brushed DC	Brushless
Maxon Part Number	118752	251601
Battery voltage (V)	24	37
No load speed (rpm)	13600	10314
Achievable stall torque (mNm)	245	670
Continuously sustainable torque (mNm)	23.1	83.1
Mechanical Time Constant (ms)	4.28	11.8
Length (mm)	54.5	20.9
Width (mm)	25	45
Mass (g)	130	110

Table 1: Motor Comparison

Nearly as important as the selection of the motor is the selection of a gearbox to accompany it. We initially chose an 18:1 gearbox as this results in dramatic, across-the-board improvements to the speed and torque capabilities of the motor/gearbox combination in X-RHex when compared to those used in Research RHex, despite boasting a slightly lower total mass (see Table 2 and Figure 4a). However, when tested in X-RHex, we found that we had to restrict motor current to each motor to 9A for thermal safety (see Section 2.2.1 for a further discussion of thermal considerations). This resulted in the torque and power characteristics in Figure 4b. Notably, restricting the X-RHex motor to 9A results in substantially lower torque and power output capacity than Research RHex at low operating speeds. This handicap manifested itself during high-torque, slow speed maneuvers such as standing up or turning in place. In order to boost torque and shift peak power output to lower speeds, we switched to a 28:1 gearbox with an identical form factor. The properties of the same motor with this gearbox are also depicted in Figure 4. The increased gear ratio ensures that we are able to supply about the same amount of torque as Research RHex at low speeds and significantly more torque than Research RHex at moderate speeds, with top speed suffering slightly. We

suspect, owing to the fact that X-RHex can generate larger torques than Research RHex until very near its no-load speed, that X-RHex will have little trouble matching Research RHex in gait speed during actual, loaded operational regimes.

Attribute	Research RHex	X-RHex 18:1	X-RHex 28:1
Gearbox Type	Planetary	Planetary	Planetary
Maxon Gearbox Part Number	166163	326659	326662
Gear reduction	33:1	18:1	28:1
Peak permissible torque (Nm)	3.4	6	6
Continuously permissible torque (Nm)	2.25	4	4
No load output speed (rpm)	412	557.5	358.39
No load output speed (Hz)	6.86	9.25	5.94
Achievable output stall torque (Nm)	8.1	9.9	15.4
Continuous output torque (Nm)	.76	1.2	1.9
Gearbox Mass (g)	162	178	178
Combination Mass (g)	292	288	288

Table 2: Motor and Gearbox Combination Comparison

The final consideration in choosing a gearbox was ensuring that the mechanical device was physically capable of withstanding the high-torques generated by X-RHex. Unlike high speed motor applications in which stall torque is rarely reached, we expect X-RHex to be approaching stall torque with regularity, demanding very large torques from each gearbox. Thus, we chose a "high-power" gearbox from Maxon's line. When compared to its ceramic alternative, the high-power gearbox increased the peak permissible torque output from 3.4Nm to 6Nm and continuously permissible torque from 2.25Nm to 4Nm. While our motor, after the gear reduction, is capable of supplying almost 16Nm of torque in stall (greatly exceeding the 6Nm limit imposed by the gearbox), our expectation is that, with a modicum of care in current limiting, we may prevent extended operation at stall and that Maxon's thresholds will never be thoroughly tested. Indeed, Research RHex has a similar conundrum: its 8.5Nm stall torque is more than double the 3.4Nm peak torque output capacity of its gearbox, yet gearboxes are damaged only very infrequently. The design specifications for the motor and gearbox combinations of Research RHex and X-RHex (with both gearbox iterations) are given in Table 2.

2.2.1 Thermal Considerations

Power density is one of the most important determinants of dynamic legged locomotive performance. Accordingly, we are strongly motivated to extract maximum power output from whichever motors we choose. The large amount of electrical power these motors consume causes heat to build up and can, if left unchecked, cause the motor coils to overheat and become damaged. However, the core motor temperature can not be measured directly: to estimate it, we build an observer in the form of a second-order lumped-element thermal model [24] using parameters given by Maxon [25]. This model is used both offline, to predict the thermal impact of a given behavior, and online, to monitor motor temperature as the robot is operating. The model is most easily visualized as a circuit consisting of two capac-

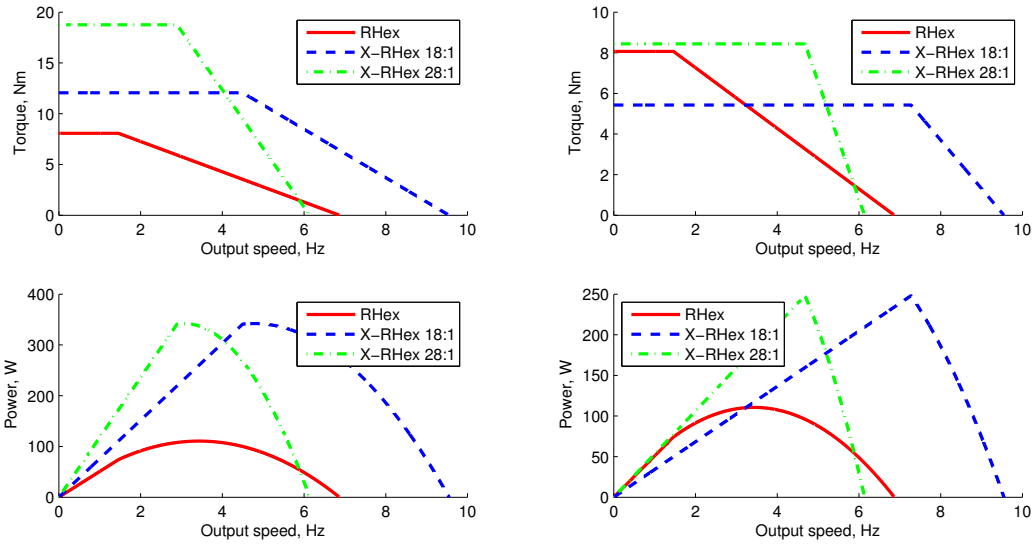

(a) X-RHex restricted to 20A, Research RHex to 15A. These values correspond to the current limits imposed by the respective motors' controllers.

(b) X-RHex restricted to 9A, Research RHex to 15A. The 9A limit placed upon X-RHex is empirically derived; above this limit we find that, in normal operation, the motors tend to heat up too quickly.

Figure 4: The output torque-speed and power-speed profiles of the three motor/gearbox combinations, for two different current limits.

itors and two resistors, a current source, and a voltage source, as pictured in Figure 5. The capacitors are referred to as "thermal masses" (C_{th1} and C_{th2}), while the resistors are "thermal resistances" (R_{th1} and R_{th2})[4]. Voltages represent temperatures, while currents denote the flow of thermal energy. Thermal resistances characterize the ease with which heat is transferred between adjacent thermal masses (in this case, different parts of the motor), while thermal masses indicate the amount of energy that is required to heat up a given motor element. The voltage source represents the ambient temperature around the motor, which is different from the unchanging reference temperature represented by ground.

The amount of power lost over the motor coils' resistance is I^2R_c, where I is the motor current and R_c is the terminal resistance. This heat source is the "input current" to our thermal circuit model. The continuous current limit given in the datasheet is actually derived from this model and the maximum winding temperature of 125°C.

Combining the thermal resistances with a motor torque constant k_M and selected gear ratio G, we can compute two derived value constants for each motor that we refer to as the "heat coefficient" for the core and case:

$$H_{core} = \frac{R_c R_{th1}}{k_M^2 G^2}$$

[4]Maxon specifies two "thermal time constants" (τ_{th1} and τ_{th2}) instead of thermal masses; these are just the thermal resistances multiplied by the thermal masses.

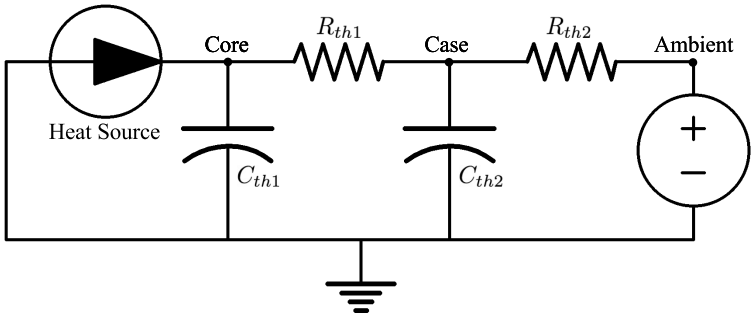

Figure 5: The thermal model represented as an equivalent circuit.

$$H_{case} = \frac{R_c R_{th2}}{k_M^2 G^2}$$

Both of these values have units of $\frac{^\circ C}{(mNm)^2}$, and can be thought of as the relative steady-state temperature rise for a given (squared) torque demand at the output of the gearbox. The first measures the temperature rise of the motor core relative to the case temperature, while the second is the temperature rise of the motor case relative to the ambient temperature — to get the temperature rise of the motor core relative to the ambient simply add the values together. These values along with the two thermal time constants completely describe the thermal properties of a given motor, and are summarized in Table 3.

Attribute	Research RHex	X-RHex 18:1	X-RHex 28:1
Thermal Time Constant Core (s)	12.4	16.7	16.7
Listed Thermal Time Constant Case (s)	910	212	212
Measured Thermal Time Constant Case (s)	551	710	710
Heat Coefficient Core $\frac{^\circ C}{(mNm)^2}$	9.9	9.4	3.9
Listed Heat Coefficient Case $\frac{^\circ C}{(mNm)^2}$	44.8	8.9	3.7
Measured Heat Coefficient Case $\frac{^\circ C}{(mNm)^2}$	17.2	10.2	4.2

Table 3: Motor and Gearbox Combination Comparison

The thermal model can be used to run a simulation of what we expect the motor's core temperature to be given a certain torque demand. As shown in Figure 6, we see that the Research RHex and X-RHex motors with 18:1 gearbox perform about equally well in the short term, with the X-RHex motor running a little cooler in the long run. This is due to the fact that they have similar core thermal constants, and Research RHex has both a higher case heat coefficient and case time constant. The X-RHex motor with 28:1 gearbox performs significantly better than either. The efficiencies of the brushless motor in the 18:1 case are almost balanced out by the better thermal characteristics of a brushed motor. Additionally, the low gear ratio means that the motor needs to generate more torque (and correspondingly more current) than an identical motor with a larger gear ratio.

The parameters supplied by Maxon are for a bare motor, and do not take into account the

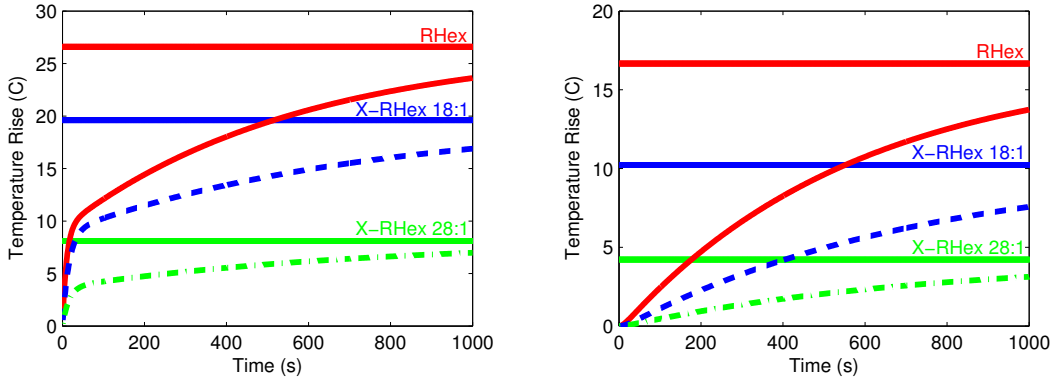

(a) Core (b) Case

Figure 6: Core and Case temperature simulations for a fixed torque demand. Horizontal lines represent steady state temperature. Note that in the short run, X-RHex with the 18:1 gearbox runs at approximately the same temperature as Research RHex

thermal effect of a gearbox. Since the gearbox is mostly metal and attached directly to the motor's case, it acts as a heat sink. To account for this, we conducted a controlled experiment to measure the thermal mass of the case and thermal resistance between the case and the air, thus assuming that the gearbox acts as an addition to the case. The gearbox could be represented separately using an additional thermal mass and thermal resistances, but we chose to employ the simple second order system as it delivered accurate empirical results during testing. We calculated an estimate for the thermal mass and resistance and used those parameters for our model. See Figure 7 for a comparison of the experimental and simulation results, and Table 3 for the numerical values[5]. The model fits the data with an RMS case temperature error of about 1°C.

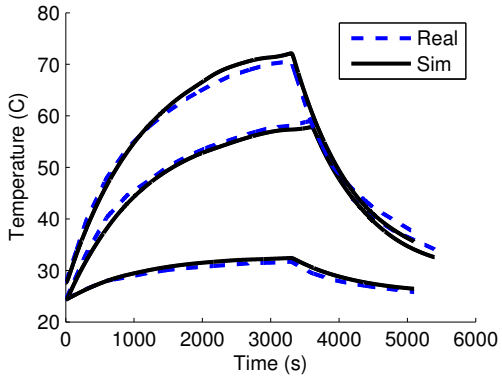

Figure 7: Comparison of measured and estimated case temperatures for three different fixed current demands followed by a cooling period (at 3300 seconds).

[5]Note that the "List" values are for a bare motor as reported by Maxon, while "Measured" were calculated by the authors and there is a slight discrepancy in some values that can be attributed to differences in methodology

There is a significant difference in the way the gearbox attaches to the motor on the brushed Research RHex motors and brushless X-RHex motors, resulting in substantially divergent thermal performance. The brushed motor coils are physically connected to the case/gearbox via bearings, brushes, and output shaft; each of these connections facilitates heat transfer between coils and gearbox. In contrast, the brushless motor coils on X-RHex are stationary, attached only to a fiberglass circuit board which acts as a thermal insulator, partially isolating the coils from the gearbox, as seen in Figure 8. As a result, while the gearbox on a brushless motor does act as a heatsink, the thermal performance improvement is substantially more pronounced when using brushed motors. Indeed, anecdotally, the gearboxes on Research RHex become much warmer than the gearboxes on X-RHex, suggesting that they are doing a better job of sinking the heat generated in the coils. The calculated thermal resistance between the case and ambient for a Research RHex motor is less than half the thermal resistance listed for a stock motor with no gearbox, while the X-RHex motor had no improvement because of the poor physical connection to the gearbox. In both cases the calculated thermal mass of the case was much more than the listed thermal mass of a stock motor. This leads to the modified τ_{th2} for Research RHex being lower than stock, while for X-RHex it is higher than stock. These measured parameters were used when generating Figure 6.

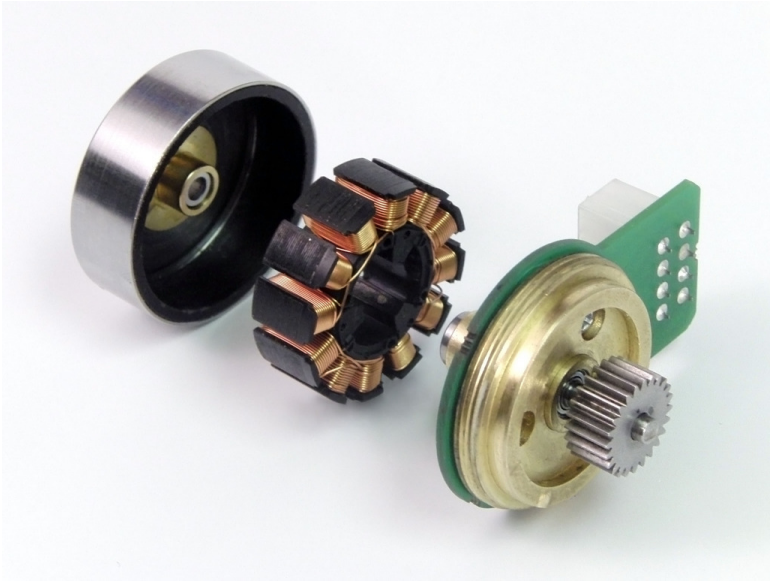

Figure 8: A disassembled view of the brushless motor.

While X-RHex motors with 18:1 gearboxes operate at slightly lower temperatures than Research RHex motors when tested on the bench (normalized for a given torque output), they run at higher temperatures on the robot. This lead us to limit the current to no more than 9A during normal operations. We are investigating multiple causes of this discrepancy, but the increase in gear ratio has substantially reduced the temperature of X-RHex motors in normal operation. Our switch from from an 18:1 to a 28:1 gearbox reduces the rise in motor temperature to achieve a given torque by 60% (as seen by taking the ratio of heat coefficients in the last two columns of Table 3).

2.3 Electrical Subsystems

The electronics of X-RHex can be conveniently decomposed into four major subsystems. A summary of the electronic infrastructure can be seen in Figure 9, and the physical layout can be seen in Figure 10. The main computer (Figure 10(a)) handles all high level control and communications. Each electronics stack (Figure 10(b)) contains three layers: motor controllers; a controller interface board which distributes power and communications to the motor controllers; and a battery management board responsible for power distribution, regulation, protection and monitoring. To the outer side of each stack, there is a lithium polymer battery and an interface board (Figure 10(c)). Finally, there is a motor assembly containing a brushless motor and related sensors at each of the six hips (Figure 10(d)).

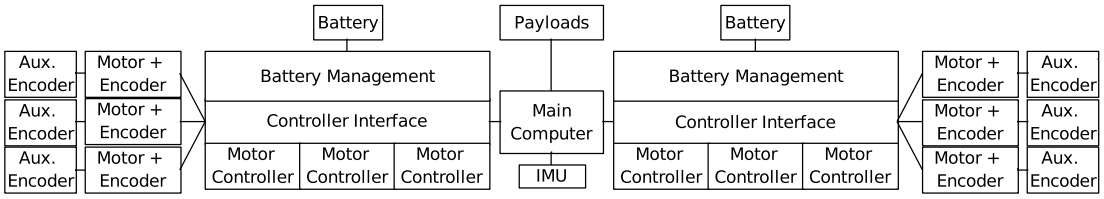

Figure 9: Structural overview of X-RHex electronics.

2.3.1 Main Computer

The robot's main computer sits near its center, in between two stacks of control electronics (see Section 3.1 for a discussion about additional computers as potential payloads). This computer controls the robot's gait and other behaviors, gathers and logs sensory data from various parts of the system, and communicates with the operator control unit (OCU). This communication is maintained via either an internal wireless card connected to the computer or an external wireless solution as a payload (For a list of modular payloads, see Section 3.1).

In addition to the sensors used in motor control and battery management, there is an Inertial Measurement Unit (IMU)[6] just below the main computer that provides inertial sensing for the robot. For a discussion about additional sensors as payloads, see Section 3.1.

Previous iterations of RHex machines, such as Research RHex and EduBot, have required larger PC/104[7] stacks to support their operation, often including PC/104 power supplies and custom interface boards for communicating with motors and sensors. Our adoption of small COTS power regulators and USB 2.0 as the communication interface removes the need for a PC/104 stack; X-RHex can operate with any USB compatible computer that meets the dimensional constraints. Currently, X-RHex is equipped with a single board PC/104 computer[8] with an Intel Atom processor.

2.3.2 Control Electronics

We use commercial off-the-shelf (COTS) motor controllers because they provide a wide range of capabilities and high performance while limiting the need for custom design, thus requiring less development time. Inspired by its success in the RiSE V3 design [13], we chose the

[6] MicroStrain 3DM-GX3, http://www.microstrain.com/3dm-gx3-25.aspx
[7] PC/104 Consortium, http://www.pc104.org/
[8] ADLS15PC, http://www.adl-usa.com/products/cpu/datapage.php?pid=ADLS15PC

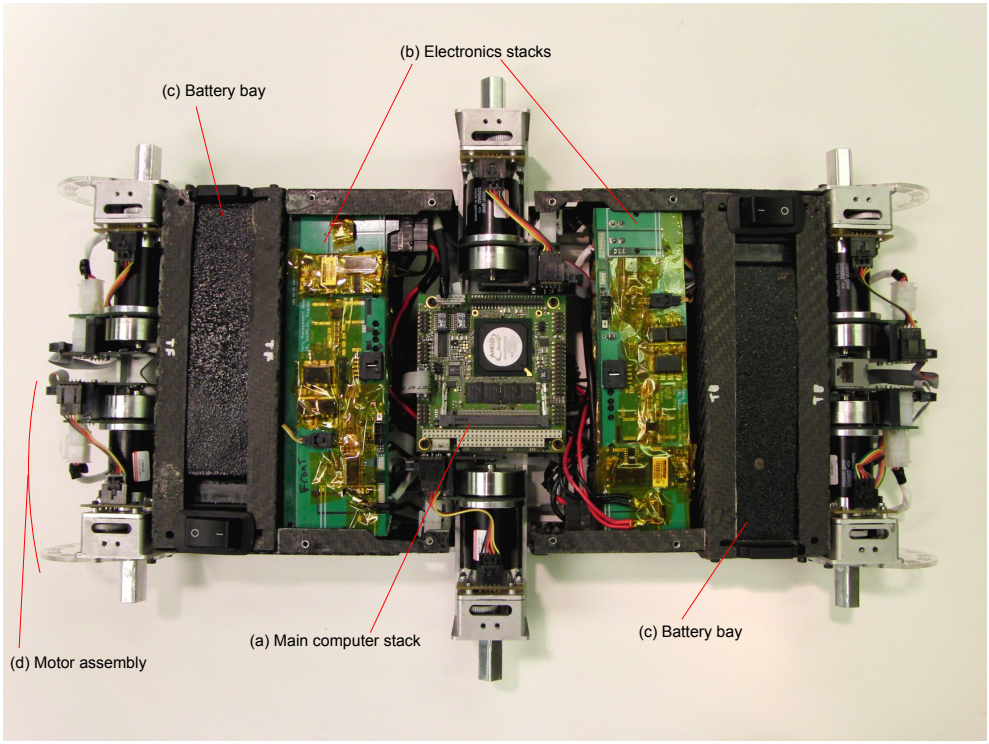

Figure 10: View of internal electronics.

Advanced Motion Controls (AMC) DZRLATE-20L080 motor controller[9]. This motor controller comes preprogrammed with a variety of control modes that allow for quick testing of control strategies with limited custom code. These control schemes include position and velocity PID-F, current, voltage, rate limiter, current limiter, PVT, and more as well as combinations of the above[10] (see [26] for details on these different control schemes). While using a COTS controller like this one saves the time and effort needed to develop the various control modes, substantial development time is required to understand and effectively use the slew of control modes provided by a third-party product.

The motor controller closes a low-level feedback loop internally at a rate of 20kHz; this high speed loop permits motor current targets to be reached rapidly and accurately. However, this low level control is inaccessible to the user, limiting the ability to add control modes to, for example, handle gravity compensation for the leg. This highlights the tradeoff between flexibility and ease of use when designing with COTS components. In addition to control loops, these controllers handle the sinusoidal commutation of our brushless motors, and provide sensor feedback for position, voltage, current, and temperature of the motor. The six motor controllers are split into two groups of three to simplify signal and power transmission while maintaining symmetry and weight balance. These motor controllers form the first layer

[9] ADVANCED Motion Controls DZRALTE-020L080, http://www.a-m-c.com/products/dzr.html

[10] We have, thus far, used three different control modes: a PD controller in position, a pure current loop, and a position-around-velocity controller. We have found the "position-around-velocity" control mode to provide the best results so far, though its functionality hinges upon extremely accurate encoder calibration (described in Section 2.3.3) and substantial parameter tuning.

of each of the two control electronics stacks.

The next layer on each electronics stack is the controller interface board that relays communication between central CPU and the motor controllers, and provides connectors for the motors and sensors. Each interface board has a high speed upstream USB 2.0 connection to the CPU that is fed into an onboard USB hub[11]. One USB channel leaves the hub for each motor controller (3 in total per board) and is then connected to a USB-serial converter and a serial-RS485 converter in order to communicate with its respective motor controller at approximately 1 Mbps. In practice, this results in full controller updates every 2.5–4 ms (depending on how much information is in each update)[12], which is much smaller than the mechanical time constant of our motors (11.5ms, not considering gearboxes or legs). This bus setup provides a robust and fast connection to the motor controllers, and allows them to be connected to any modern computer over USB. We designed a board for this task, as there was no COTS solution to interface our specific motor controllers with a USB-based system. The schematic for this board is based on the reference designs for the motor controllers, USB hub chip, and serial interface chips.

The top layer of the stack (above the controller interface board) is a battery management board. Each battery management board is connected to a 10-cell lithium polymer battery. The board has a dedicated protection IC monitoring voltage levels of individual battery cells in addition to the current flow at the negative terminal of the battery. In case of a fault such as a short circuit, the protection IC powers down the robot. This board also contains COTS voltage regulators for electronic components requiring lower voltage levels — each board provides 5V and 12V DC power. Each battery management board is connected to the CPU and reports voltage and current draw for each battery independently via the USB hub on the proximal controller interface board. This board is the most extensively custom element of the electronic system, since no suitable off-the-shelf product could be found that worked with our system specifications. The schematic for this board is based on the reference designs for the protection chip, MCU, and serial interface chips. This board is described in more detail in Section 2.3.4.

2.3.3 Motor Assemblies

Each motor assembly is connected to a controller interface board via two cables. The first carries power to each of the three motor windings, and the other carries all of the low voltage signals including encoders, hall sensors, user LEDs, and the temperature sensor. The sensor cable connects to a primary encoder board mounted on the back of the motor. This board has the primary encoder IC, a 10-bit, 3-channel magnetic encoder (which must be aligned as accurately as possible over the center of a diametrically polarized magnet mounted on the back of the rotating motor case), and the temperature sensor measuring the ambient temperature next to the motor (see Section 2.2.1 for how this is used). It also connects to the hall sensors located inside the motor. Lastly, this board has a cable connection to the auxiliary encoder board located next to the secondary output shaft. By providing an absolute measurement of the leg angle, the auxiliary encoder removes the need to calibrate the motor when starting the robot (see Section 2.1.2 for mechanical details). Lastly, this auxiliary encoder board externally displays two user controlled LEDs.

[11] Universal Serial Bus Community Website, http://www.usb.org

[12] As measured by taking the average difference between the system timestamps of consecutive iterations

2.3.4 Battery Power

One major challenge in designing highly mobile platforms is to select a battery solution that is capable of providing enough power at high discharge rates and still has enough capacity to maintain operation for long periods of time without any interruption. X-RHex uses lithium polymer (LiPo) batteries. LiPo batteries were chosen because of their high energy-to-weight and energy-to-cost ratios and charge-discharge efficiency [27, 28]. One major advantage of this battery type is the flexibility in form factor. Cells can be built in different shapes and sizes, with battery packs composed of several cells connected in series. Thus, manufacturers have significant control over the final shape of the whole pack. Indeed, as a popular option in RC model airplane and car design, there are LiPo batteries available in a wide variety of capacities, voltage levels and shapes[13].

Voltage is perhaps the most important factor for our battery selection. We have weighed the advantages of high voltage systems (higher speed and power in motor operation and lower power losses in cabling) against the disadvantages (fewer battery options, more expensive electronics, and reduced availability of COTS battery protection solutions). With this in mind, we have chosen a LiPo battery with a nominal voltage of 37V (42V at full charge), which is relatively high while still commercially available, easy to integrate into our system, and safe to handle[14].

Based on our design specifications, the battery chosen for X-RHex is a 10-cell (37V) pack with 3900mAh capacity(C) and 20C (78A) continuous, 40C (156A) burst maximum discharge rate[15]. The energy-to-weight ratio of this selection is around 164 Wh/kg, and the continuous power-to-weight ratio is around 3200 W/kg.

Lithium polymer batteries require careful handling and monitoring because of their volatile nature. Under faulty operating conditions like over-discharge or improper voltage levels, the cells may be damaged irreversibly, and even catch fire. Monitoring and handling have to be performed at the cell level since homogeneity both in charging and discharging phases is not guaranteed. A commercial cell-balancing solution can be used for charging, but embedded monitoring is needed during discharging [30].

In our design, a commercial integrated circuit[16] is used to monitor the voltage level of individual cells, implementing a state machine that is responsible for detecting faulty operating conditions. To be able to transfer and log necessary information about state of the battery, a micro controller unit (MCU) has been added to the system. The MCU acts as a host and, although the integrated circuit has absolute control over emergency situations, the final decision about going back to normal operation scheme is made by the MCU. This MCU communicates back to the main computer over USB through the controller interface board (see Section 2.3.2).

One important feature of the X-RHex battery system is the ability to replace discharged batteries with fully-charged ones without any interruption in robot operation. Our design makes this possible by using Schottky diodes on both battery management boards acting as an "OR" switch on the high voltage line. Thus we are able to connect two batteries in parallel and replace one at a time without any interruption in power or damage to either battery.

[13] Thunder Power RC http://thunderpowerrc.com/, DragonFly Innovations Inc. http://www.rctoys.com/

[14] An adult male faces risk of injury at currents above 62mA. Using an approximate "sweaty-palm" resistance of 1000Ω, the maximum "safe" voltage level for short term contact is 62 VDC. Our choice of a bus voltage of 37–42V allows for a 1.5x safety margin for transients caused by dynamic system loads [29].

[15] Thunder Power TP-3900-10SPL2, http://thunderpowerrc.com/

[16] Texas Instruments BQ77PL900, http://focus.ti.com/docs/prod/folders/print/bq77pl900.html

2.4 Software Architecture

X-RHex makes use of a real-time software architecture to provide high frequency sensing and control, as well as network communication with the robot, on a near-stock Linux distribution[17]. Our software architecture is based on a custom-developed open source package called *Dynamism*[18].

Dynamism is a software library, implemented in C, consisting of a real-time distributed database that facilitates the sharing of data amongst multiple networked computers. Compared to systems such as ROS [31], Player [32], and others, Dynamism is designed specifically as a lightweight library for real-time tasks and is intended for lower-level control than typically performed with most robotics software. Dynamism also provides some useful utilities such as a logging interface that can be used with any data registered within the distributed database. Each program running Dynamism can register data within the database, allowing other Dynamism programs to easily access and modify the data as need be in a peer-to-peer network model. To work well with robotics application such as controlling a RHex robot, the database elements are read and written at real-time rates, often within a single process on the robot's CPU, but also by any other machines sitting on the network.

Prior RHex robots utilize a different real-time control package, *RHexLib*[19], a C++ package containing a class-based control architecture in which individual robot components are implemented as modules with defined interfaces. Sharing of information between modules within the same control process takes place through class methods for each component. Network control, however, is performed using a separate system that implements a client-server architecture between the robot and a single operator control unit (OCU), with specifically chosen control modes and variables exposed through the communication protocol.

In comparison, Dynamism routes all data communication through the real-time distributed database. Within a single robot process, control is similar to RHexLib, only replacing the C++ class methods with reading and writing of database entries. The advantage of the real-time database is that, with the network interfaces that Dynamism provides, any robot data may be accessed from other processes on the robot or other computers on the network, thus eliminating the need for a separate network protocol to communicate with an OCU or other robots. Dynamism, thus, allows control to be performed from within a single process, amongst multiple processes, or amongst multiple computers, all with very few code modifications. Dynamism additionally provides profiling of control code and network latency, in order to assess the rates at which control is possible in different networked configurations.

One additional feature of Dynamism is the inclusion of language bindings for scripting languages such as Python[20] and MATLAB[21], thus making it possible to access robot data and issue control commands from a scripted application or interactive console. The MATLAB binding is implemented as a compiled `mex` program, written in C, that translates MATLAB function calls into Dynamism calls. The Python binding takes advantage of the `ctypes` package, thus allowing native Python code to execute functions within Dynamism's shared library. With minimal changes due to syntax differences of the various languages, all three programming interfaces use the same function calls, and code can be ported amongst them with relative ease. Additionally, the lightweight interface used by Dynamism has allowed easy

[17] Ubuntu Linux, http://www.ubuntu.com/
[18] Dynamism, http://www.dynamism-project.com/
[19] RHexLib, http://rhex.sourceforge.net/
[20] Python, http://www.python.org/
[21] MATLAB, http://www.mathworks.com/

integration with external robotics software, such as ROS [31].

The X-RHex interface and control code, `xrhex_software`, contains code for the motor controllers, battery management boards, a variety of sensors, and robot behaviors. Each component consists of a self-contained library, typically written in C, with a small set of code to interface with data from the Dynamism database. While developed with the X-RHex robot, this software has been backported to work with previous RHex robots, such as Research RHex and EduBot, thus allowing the use of shared software and behaviors amongst all three platforms. In addition, the robot software takes advantage of the scripting language bindings by storing configuration data and some control commands within Python scripts, including separate configuration scripts for individual platforms, robots, and experiments.

Though the robot software is typically executed within a single control process on the robot, Dynamism allows robot programmers to rapidly prototype behaviors from separate processes, often executed off of the robot. Furthermore, with a distributed architecture, a variety of client-side debug applications, including simple graphical user interfaces and visualization applications, have been implemented in MATLAB, Python, and C.

3 Payloads and Applications

Development of advanced sensor-based behaviors on a portable, highly-dynamic legged robot is a primary goal of the X-RHex project. While essential sensors (motor and battery feedback sensors and an IMU) have been designed into the body of the robot, the choice of additional sensors largely depends upon robot activity, yet the specifications of a desired sensor package may vary with changing research needs and advancing sensor technologies. To address this issue, we introduce a modular payload architecture that allows X-RHex to perform as a *laboratory on legs*; a user may easily change payloads to rapidly develop behaviors in natural, outdoor environments as easily as on a lab bench. These sensors will be used to better understand properties of the robot's dynamic locomotion as well as its external environment. X-RHex has been tested to navigate basic terrain successfully with up to 12 kg of payload weight — more than enough for any planned computational or sensory payload (no heavier weights have been tested, yet). In this section, we introduce the payload system and describe several application scenarios we intend to pursue.

3.1 Modular Payload System

X-RHex is equipped with two Picatinny rails [33] as a universal payload mount. While commonly found on handheld weaponry, Picatinny rails have been adopted by robots such as DragonRunner [34] and PackBot [35], among others. On X-RHex, two parallel rails, 40 cm long and spaced at a center-to-center distance of 14 cm, span the length of the body. Payloads equipped with Picatinny mounts can be placed on a single rail (off-center) or with mounts spanning both rails.

In addition to a standardized mechanical mount, X-RHex provides an electrical interface to sensors and payloads through a series of standardized connectors placed on its top frame. These include power connectors capable of delivering various voltages to payloads, providing up to 2A at 5V, 2A at 12V, and 4A at battery voltage (37-42V), all generated by the X-RHex battery management board (Sec. 2.3.4). Multiple USB connectors and an Ethernet port allow direct connections between payloads and the robot's on-board computer. Fig. 11 shows an example configuration of the X-RHex robot carrying a variety of payloads.

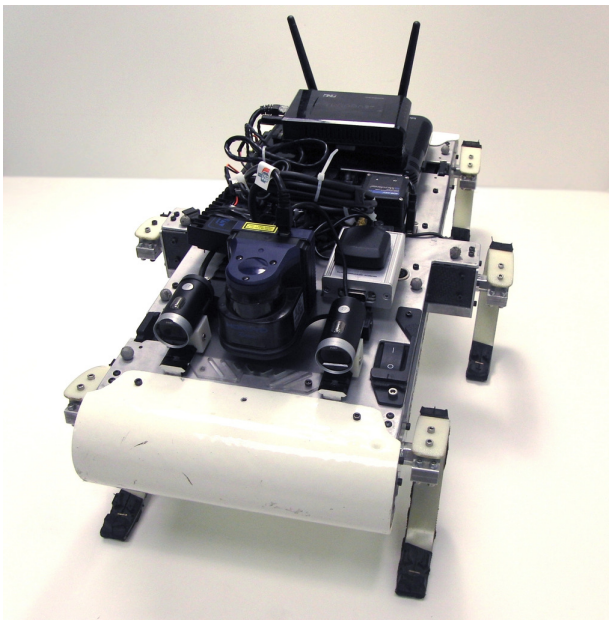

Figure 11: X-RHex outfitted with multiple payloads.

The following sensors and payloads have been equipped with Picatinny rail mounts for convenient modular use on X-RHex:

- A variety of commercial webcams that can be used for teleoperation scenarios or image processing[22].
- A set of three webcams that are used to create a panoramic teleoperation view.
- A GPS unit, including antenna, that provides position data to the robot in outdoor environments[23].
- An external IMU, used in replacement or in addition to the internal IMU[24].
- A LIDAR unit to get a line-scan point cloud of the space in front of the robot[25].
- A secondary computer with onboard GPU for fast parallel processing of sensor data, along with a DC-DC converter to supply the 19V power required[26].
- A wireless IEEE 802.11n access point for increased communication range over our traditional use of 802.11b/g wireless adapters[27].
- A USB Hub and USB flash storage devices.

[22] For example, Microsoft Lifecam Cinema, http://www.microsoft.com/hardware/digitalcommunication/productdetails.aspx?pid=008

[23] U-Blox EVK-5H, http://www.ublox.com/en/evaluation-tools-a-software/gps-evaluation-kits/evk-5h.html

[24] Microstrain 3DM-GX2, http://www.microstrain.com/3dm-gx2.aspx

[25] Hokuyo URG-04LX-F01, http://www.hokuyo-aut.jp/02sensor/07scanner/ubg_04lx_f01.html

[26] Lenovo IdeaCentre Q110 Mini PC, http://www.lenovo.com

[27] TRENDnet TEW-638APB, http://www.trendnet.com/products/proddetail.asp?prod=140_TEW-638APB

- A pair of COTS Picatinny handles, designed for use on weaponry, but easily used as carry handles for the robot[28].

In addition to the sensors and payloads mentioned above, we intend to pursue other payloads in the future, such as auxiliary batteries to increase the robot's run-time, as well as additional actuators, such as a small robotic arm atop the robot.

With the secondary computer attached, we claim X-RHex to be the first robot of its size (under 10kg with payload mounted) to carry a programmable GPU. In recent years, programmable graphics hardware has been used to speed up computation in problems like image segmentation [36] and path planning [37], among others. The desktop GPUs which have become the mainstay of the computer graphics and research communities are too large and too heavy to meet the constraints of untethered mobile robotics. However, the small, low power variants of these produced for laptops and nettops are much more suitable for power and weight constrained applications. The payload computer shown attached to the robot in Figure 11 has a 16 core nVidia GPU capable of running CUDA [38], a programming and computing architecture that allows highly-parallel execution of machine code, while adding only 0.65kg to the system weight. The computational power of this secondary computer will be used to process sensor data in a parallel fashion, independent of the internal computer. Specifically, we plan to extract SIFT [39, 40] and SURF [41, 42] features in real time using GPU implementations of the algorithms, in order to perform feature extraction, tracking, and optical flow calculations during dynamic locomotion.

3.2 Applications

The modular payload system permits researchers to switch, with minimal downtime, between distinct experiments that use the same mobile platform. Here we describe several existing applications, as well as future application scenarios we envision.

Significant effort has been applied to evaluating RHex-like robots' gaits for the purpose of improving locomotion efficiency. X-RHex is capable of automated gait tuning using a variety of exteroceptive feedback modalities. A critical challenge for automated tuning is the localization of the robot within its environment while evaluating the electrical power consumed [20]. Previous work has utilized an on-board camera to track features in a structured environment [43], an extremely accurate indoor commercial motion capture system [44], and, most recently (with the X-RHex robot), a GPS payload in unstructured outdoor environments. Each tracking method offers advantages and disadvantages, and the modular payload system allows X-RHex to perform gait tuning in a wide range of scenarios.

There is an ongoing effort to develop accurate state estimation for RHex using proprioceptive and vestibular sensors, such as an IMU or leg encoders ([45, 46] among others). Tasks such as performing automated gait adjustments [47, 48], choosing gaits based upon changing surface properties [49], or recovering from a fault such as a broken leg [50] are all intended uses of an improved state estimation capability. X-RHex's payload system is primarily geared toward exteroceptive sensing, which we believe can augment and expand the current work in state estimation. As an example of some potential applications, on-board cameras, along with additional computational power of a payload computer, can be used for measuring optical flow or performing stereo vision, both of which are useful to estimate the robot's motion within an environment. A planar laser scanner, coupled with the natural dynamic bouncing

[28] Tippmann M16 Carry Handle - X7, http://www.tippmann.com/usa/product_guide/accesDetails.aspx?id=131

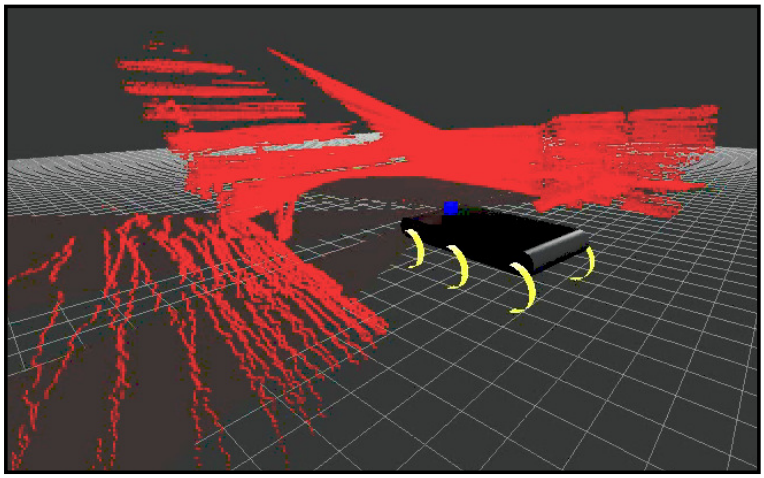

Figure 12: Using the internal IMU and a payload laser scanner, X-RHex can create a 3D point cloud of its surroundings.

of X-RHex during locomotion could be used to construct a 3D point cloud representation of the environment, as shown in Fig. 12. Cameras and laser scanners could also be used in combination with proprioceptive information to build a terrain classifier.

RHex robots have relied primarily on their morphology, mechanical compliance, and offline-tuned controllers to provide stability in a purely feedforward gait context [51] (see [52] for biological evidence that mechanical structures also provide stability in animals). To further increase stability and efficiency across varying environments, rapidly updated pose and terrain information will facilitate the development of algorithms that adjust the robot's gait based upon terrain type and sensed obstacles in its path. While most existing legged robots are roughly divided between those that plan each specific stride and foot placement [53, 54] and those that employ pre-generated, time-parametrized gaits (either through mechanical [55] or control [48] methods), the X-RHex robot has the potential to facilitate the bridging of these two divergent approaches.

The scaling of higher forms of robot autonomy down to a small legged platform is an additional direction of research made possible by the X-RHex platform. While there exists a rich literature of autonomy approaches for large outdoor wheeled vehicles, such as within the scopes of the DARPA LAGR [56], Grand Challenge [57], and Urban Challenge [58] programs, the ready application of this work to small legged machines in outdoor settings is an open challenge. Initially, this work will focus on the collection of datasets recording the sensorium of a small, rugged, legged robot traversing — and bouncing through — complex terrain, in order to study methods of sensor fusion and state estimation. With improvements in sensing and computational power, however, autonomous behaviors such as those developed in the above programs can be applied to the X-RHex machine.

4 Comparison with Prior RHex Robots

In this section we compare X-RHex with prior RHex-like robots[29], with a focus on Research RHex [1], but also considering Rugged RHex [7, 8, 9] and EduBot [10, 44]. Each of these platforms was developed through multiple iterations — differences between these versions account for the range of values presented for certain parameters. This section is not intended to demonstrate the superiority of any one platform; instead we aim to highlight the similarities and differences between platforms.

4.1 Mechanical

Each RHex robot was designed with physical dimensions determined by the proposed usage of that platform. Edubot is a smaller and more economical RHex variant, while Rugged RHex is larger and more powerful than the original. The scale of Research RHex has proven to be an excellent compromise and suitable for both the laboratory and field; its inter-leg distances and frame geometry make it adept at traversing obstacles (including stairs), while still being small enough and light enough to be easily carried by a single person. X-RHex was designed with size and mass similar to Research RHex to capitalize on these advantages of scale. A thorough comparison can be seen in Table 4.

Attribute	Research RHex	Rugged RHex	Edubot	X-RHex
Body Height (cm)	12–13.9	14.8	6.3–10.8	7.5
Overall Width (cm)	39	46.5	34	39
Body Length (cm)	54	62.3	36	57
Leg to Leg Spacing (cm)	20	23.5	15.5	22
Ground Clearance (cm)	11.5	10.6	7–9	12.5
Inverted Ground Clearance (cm)	9.5	10.6	N/A	12.0
Leg Diameter (cm)	17.5	19.5	10.8–11.7	17.5
Total Weight (kg)	8.2–8.9	15	2.5–3.6	8.6–9.5

Table 4: Comparison of Physical Properties.

Using Research RHex as a basis for comparison, the X-RHex frame was intended to improve upon its predecessor's mechanical properties while occupying a similar footprint. From the standpoint of frame stiffness, Research RHex suffers from a lack of support on the top of its motor mounts. This lead to an underutilization of the upper frame elements as the legs — particularly the middle legs — are loaded. A static stress analysis is depicted in Figure 13. Note the very low stress concentrations experienced by the upper members of the Research RHex frame relative to the cross pieces on which the motors are mounted. The X-RHex frame uses the motor mounts as rigid blocks that serve to connect a strong top and bottom structure, greatly increasing the overall stiffness of the frame in both the lateral and longitudinal directions. The X-RHex frame also derives far superior torsional (or rotational) stiffness from the generally greater cross section along the length of the frame (due to the monolithic nature of the top plate, the increased cross section of the runners, and the addition of Picatinny rails).

[29]There is insufficient information available to provide a comparison to the SensoRHex [12] or AQUA [11] platforms.

In addition the Picatinny rails lend a surprising supplement to longitudinal stiffness (Table 5). Stiffness is also improved between X-RHex and Research RHex by the use of 7075 aluminum alloy as opposed to 6061 alloy.

Stiffness Attribute	Research RHex	X-RHex	X-RHex / Research RHex
Lateral Stiffness (kN/m)	51.60	242.3	4.696
Longitudinal Stiffness (kN/m)	32.16	115.1	3.579
Rotational Stiffness (N/rad)	14.09	73.98	5.252
Torsional Stiffness (m^4/rad)	1.142E^{-8}	7.564E^{-8}	5.331

Table 5: A comparison of frame stiffnesses. Similar static loads were applied in each direction to generate a relative stiffness comparison. While still representing the overall strength and life time of each frame, no thorough cyclical loading or drop analysis have been run on either frame yet.

Impact resistance, both from debris and from dropping, is perhaps the most important mechanical characteristic of a RHex robot frame. EduBot was designed for lab use and other very little consideration to possible impacts by foreign debris or dropping is given. Since Rugged RHex was specifically designed for harsh outdoor use, it is fully protected against impacts but is also much larger and heavier than the size desired for X-RHex. Finally, Research RHex has been equipped with many different coverings, all of which share some common weaknesses. The shell and side plating on Research RHex provide little protection from direct impacts. As a result, the Research RHex frame has been warped or badly dented by such impacts. Also, the motor controller heatsink on Research RHex is exposed through the side plating, causing it to break off of the rest of the shell when it when exposed to an impact with the environment.

In contrast to Research RHex and EduBot, the composite plating and shell on X-RHex were designed to fully protect the internal components of the robot and to form a barrier between obstacles or debris and the base aluminum frame of the robot. The composite material used is strong enough to survive taking the full impact of the robot with the ground (or large debris) for falls from low heights (or movement at moderate velocities).

The serviceability of X-RHex was the final major factor influencing design decisions. While EduBot, with its minimal shell, can be easily serviced, the service or replacement of Research RHex internal components requires removing and then reassembling most of the robot's interior or even part of the frame. Only motors and motor mounts are an exception — these can be removed with minimal disassembly. X-RHex provides increased ease of serviceability for internal components within a platform that is fully protected. Internal components are grouped into modules such as motor assemblies and motor controller stacks. Any such internal unit can be accessed and removed by taking off the bottom shell and removing 4–6 screws. This ease of access is more than a convenience; we expect X-RHex to experience reduced down-time as its components can be repaired or replaced much more rapidly.

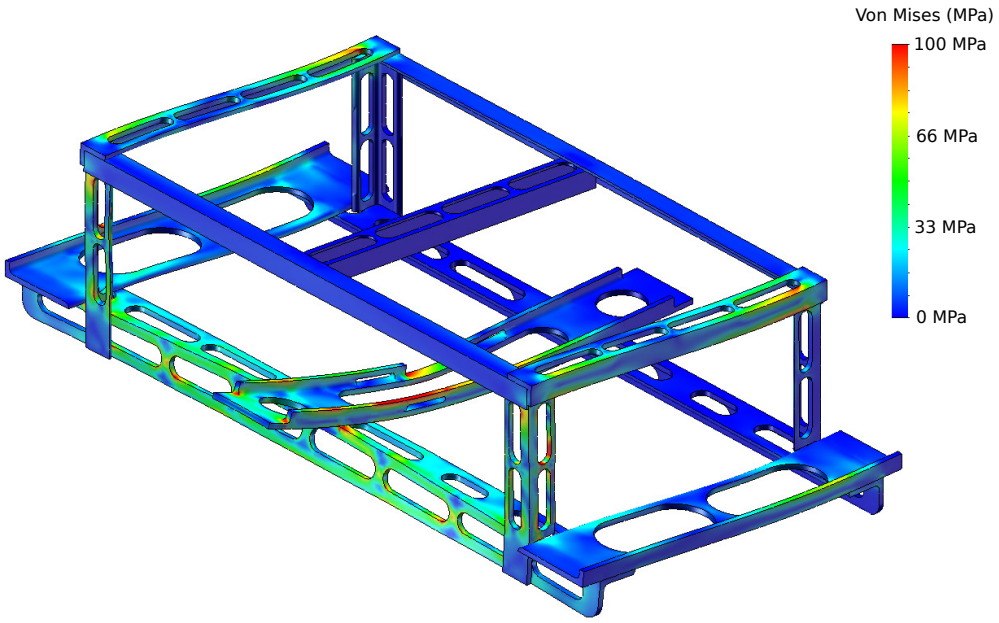

(a) Research RHex stress magnitudes

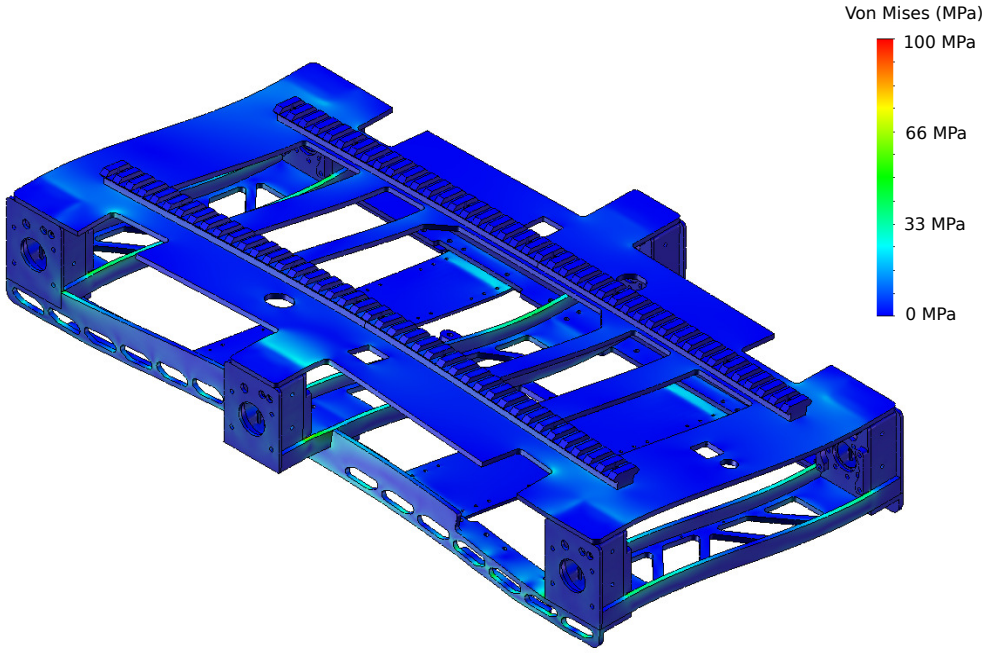

(b) X-RHex stress magnitudes

Figure 13: An illustrative comparison of stress reactions to static loading on the middle leg. The load applied (250 N) and the color scale are identical.

4.2 Energy and Power Density

In addition to physical design parameters discussed above, factors such as motor power density, thermal properties, and power-to-speed profile [59], are of critical but still imperfectly appreciated and poorly understood importance in mobile locomotion. This has been well documented in robotics [60], biology [61], and bioinspired robotics [62], for decades. A motor power density comparison amongst various RHex-like robots is certainly important, though the procedure for comparing power densities across platforms which operate at different voltage levels and velocity ranges has not been thoroughly developed in any literature to the best of our knowledge. In Table 6, we report on four distinct, crucial aspects of power density in RHex variants. We look at either continuously achievable power output (a reflection of the robot's steady-state capability) or absolute maximum motor power output (an indicator of the robot's peak dynamic capability, e.g. a single leap). We determine the motor power density by dividing power output by the combined mass of motor and gearbox (an indication of technological progress by the motor manufacturer) and determine the robot power density by dividing the total power outputs of all six motors by the robot's entire mass (a better indicator of the robot's overall capability). All parameters are taken from the motors' specifications and adjusted for each robot's respective operating voltage (as described in Section 2.2). The high voltage supply and light weight of the X-RHex motor is clearly reflected in its power density values; it achieves dramatically higher motor and robot power densities for both continuous and peak operation than its predecessor. Power density is not the only important factor, as gearing must be appropriately chosen to allow the motors to achieve these power values. However, these values do demonstrate the advantages of brushless technology and high-voltage supplies in terms of power density.

Attribute	Research RHex	EduBot	X-RHex
Motor Type	Brushed	Brushed	Brushless
Listed Motor Power (W)	20	11	50
Gear Ratio	33:1	24:1	28:1
No-Load Speed (Hz)	6.86	6.45	5.95
Encoder Type	Optical	Optical	Magnetic
Encoder Precision (cnt)	500	512	1024
Leg Calibration Sensor	Hall	None	Absolute Encoder
Other Motor Sensors	Temp.	None	Current, Voltage, Temp.
Motor and Gearbox Mass (g)	292	126	288
Max Power Output (W)	111	17	342
Cont. Power Output (W)	30	9.9	84
Max Motor Power Density (W/kg)	380	135	1190
Max Robot Power Density (W/kg)	78–84	28.2–40.8	216–240
Cont. Motor Power Density (W/kg)	103	79	292
Cont. Robot Power Density (W/kg)	20.4–22.2	16.8–24.0	52.8–58.8

Table 6: Comparison of Motor Properties. Rugged RHex uses 70W brushed motors, however the remaining parameters are not available and its column has been left out. Note that while motor power densities are listed for an individual motor, the robot power density compares the sum of all 6 motors to the entire robot mass (such as during a leaping task).

While motor power is critical, it must be supplied by an appropriate power source. Research RHex is powered by Nickel-Metal Hydride (NiMH) batteries; three battery packs are connected in series to reach the desired bus voltage level. Both EduBot and X-RHex are powered by Lithium Polymer (LiPo) batteries. Battery selection for Research RHex reflects the technology available a decade ago. At that time, LiPo battery technology was not mature enough to be widely used by the robotics community. Despite lower power density (as seen in Table 7), NiMH batteries do have some distinct advantages over LiPo batteries. First, NiMH batteries are more widely available and substantially less expensive. Moreover, unlike LiPo batteries, NiMH batteries do not require advanced protection solutions since they are not irreversibly damaged when drained below a threshold voltage. As a result, Research RHex needs only a fuse for short circuit protection. LiPo batteries, on the other hand, may be irreversibly damaged or catch fire if mistreated electrically. Thus, platforms which use LiPo batteries must include battery protection circuitry; EduBot contains a simple battery under-voltage protection, while X-RHex relies on a commercial IC to detect and handle problems, including over-discharge rate, short circuit, and under-voltage. Discussion on some of the advantages of LiPo batteries and a more detailed description of battery management on X-RHex can be found in Section 2.3.4.

Attribute	Research RHex	Rugged RHex	EduBot	X-RHex
Battery Type	NiMH	NiMH	LiPo	LiPo
Bus Voltage (V)	24	48	14.8	37
Battery Capacity (Wh)	72–120	86.4	20–30	144
Battery Quantity	1 set of 3	1 set of 2	1–2	1–2
Battery Dimensions (mm, each)	157x47x25	127x112x63	66x27x34–50	136x70x43
Battery Mass (g, each set)	1200–1475	1760	122–160	880
Robot Mass Dedicated to Batteries (%)	14.6–16.6	23.4	3.6–8.9	10.2–18.5
Battery Energy Density (Wh/kg)	60–81	49	316–370	328
Robot Energy Density (Wh/kg)	8.1–13.5	11.5	5.8–16.7	16.7–30.3

Table 7: Comparison of Battery Properties. Rugged RHex is assumed to use its two batteries in series.

4.3 Electronics

More than just differences in motors and batteries, the electrical system as a whole is very different between the various platforms, as shown in Table 8. While the main computer on Research RHex runs both high level gait regulation and low level feedback loops, X-RHex uses a distributed architecture (as did EduBot) with a dedicated off-the-shelf module to control each motor. This allows the innermost control loops to run much faster (20kHz on X-RHex vs 1kHz at Research RHex), improving the controller's ability to maintain specified currents.

Attribute	Research RHex	EduBot	X-RHex
CPU Type	AMD Geode	AMD Geode	Intel Atom
CPU Speed (MHz)	233–300	233–333	1600
Operating System	QNX	Linux	RT Linux
Motor PD Loop Location	Central	Distributed	Distributed
Motor PD Loop Speed (Hz)	1,000	1,000	20,000
Gait Regulation (Hz)	1,000	150–200	300
Internal Bus Communication	None	I^2C	USB

Table 8: Comparison of Computation Properties. The properties of Rugged RHex are not available and its column has been left out.

In order for X-RHex to use this distributed architecture, there must be a reliable communication network to relay information between the low- and high-level controllers. X-RHex uses USB which allows any modern computer to simply plug in and be able to communicate with all of the connected devices. EduBot uses a custom protocol built on top of an I^2C bus[30]. However, this has proven to be somewhat unreliable and susceptible to bus noise. In addition, a fully-custom bus-interface board is needed to relay CPU communication over the bus. Research RHex, as noted before, performs all calculations on the central CPU and does not require an internal network. The minimalist architecture of Research RHex permits faster CPU update rates, resulting in fast high level gait control update rates (0.3 kHz bus update on X-RHex vs 1kHz update rate on Research RHex).

While almost all RHex robots have provided battery voltage and current feedback to monitor charge level and power draw, X-RHex is the first to provide per-motor sensing of voltage and current. While bus voltage is approximately the same from motor to motor, local current sensors provide a much better understanding of how much torque individual motors are producing. Past research has used virtual sensors to approximate this [3, 50], however these methods can be enhanced (although likely not completely replaced) by the current sensor.

Owing to the differential encoders used on each platform, leg angles must be calibrated upon robot startup. Research and Rugged RHex use a hall effect sensor and a magnet on the leg to measure when the leg reaches a certain calibration position. EduBot (as well as any RHex robot in the case of sensor failure) rotates its legs back until its toes touch the ground, providing a fixed angular reference when performed on flat ground. However both of these methods require the robot to move its legs from unknown starting positions to reach a pre-determined calibration angle. While this may be acceptable in a laboratory setting, it is generally undesirable, and may even not be possible when the robot is on uneven terrain or in a crowded environment. Therefore X-RHex was designed with an absolute encoder to directly measure the output leg angle, without having to go through any sort of calibration behavior (see Section 2.1.2 for a discussion of how this is achieved).

4.4 Locomotion

Due to improvements in both motor power density and overall energy density over prior RHex platforms, we expect X-RHex to demonstrate improved performance across a variety

[30] I^2C specification, http://www.nxp.com/acrobat/usermanuals/UM10204_3.pdf

of behaviors. Its increased energy and power densities should result in increased run-time and allow X-RHex to exceed previous platforms' dynamic capabilities during short-duration, high-power-output tasks (e.g. leaping, climbing over large rubble).

Through preliminary tests, X-RHex's power efficiency has been comparable to its predecessors'. Using a hand-tuned gait on a flat linoleum floor, the robot (mass of 8.93kg at the time of testing) consumed an average of 104 W (including a hotel load of 31 W) while traveling at roughly 1.2 m/s. This corresponds to a specific resistance value of 0.90 (0.64 without the hotel load). While this specific resistance is 25% higher than that of Research RHex, that robot's fastest and most efficient gaits were developed through an automated tuning procedure [20], and we expect that the application of automated gait tuning will substantially improve the initial performance findings of X-RHex as well.

A brief comparison of various robots' locomotive performance is shown in Table 9.

Attribute	Research RHex	Rugged RHex	EduBot	X-RHex
Running time, typical usage (min)	60–80	90	20–40	90–180
Top speed (m/s)	2.7	1.2	2.5	1.54
Top speed (bodylengths/s)	5	1.9	6.9	2.7
Range (km)	3.7	4.8	*0.5*	*12*
Best specific resistance	0.72	0.80	0.5	0.90

Table 9: Comparison of locomotion properties. Running times are approximate and dependent on usage patterns and robot configuration. Italicized range distances are computed; all other values were experimentally derived. Performance values for X-RHex are preliminary and have not been thoroughly explored.

5 Conclusions and Future Work

We have presented an overview of the design and development of X-RHex as well as a comparison of its mechanical, electronic, and software infrastructure to previous RHex-style machines. We have also introduced the motivating concept of a *laboratory on legs* and have discussed several possible outdoor applications.

The greater power and energy density of X-RHex will improve its dynamic capabilities when compared to previous platforms, and the COTS electronic infrastructure allows for near plug-and-play sensor incorporation. With the payload computer attached, X-RHex is the first robot of its size to support a programmable GPU that will meet the computational demand of a variety of sensors. Together these characteristics make X-RHex an ideal testbed for nontrivial sensorimotor tasks, in which sensory information may be used to improve the dynamic capabilities and high-level intelligence of a robust legged platform in interesting terrain, as in Figure 14.

Future work with X-RHex will include a formal analysis of its locomotive properties along the design points we have discussed; by analyzing the robot's efficiency, run-time duration, and dynamic capabilities, we can gauge the effectiveness of our design choices. We will also utilize our growing assortment of sensory payloads to build new sensor-based behaviors for RHex robots.

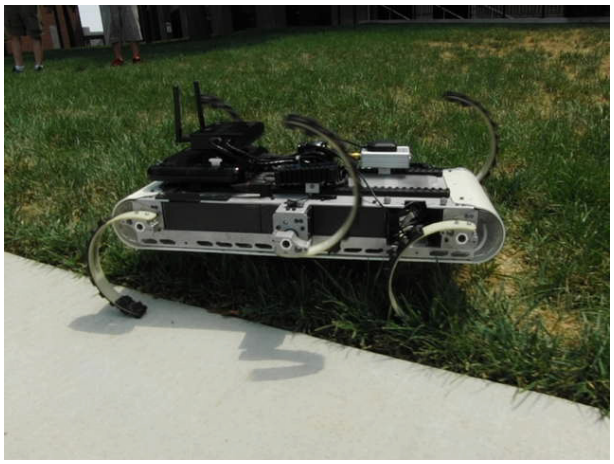

Figure 14: The X-RHex robot with a variety of payloads in an outdoor environment.

Acknowledgments

The authors would like to thank Earvin Caceres and ADVANCED Motion Controls for their help and support; Dr. Haldun Komsuoglu and Dr. Shai Revzen for numerous useful consultations and stimulating discussions; Aaron Peck and Matthew Hale for help building the robot; Gina Burgese for her assistance with the logistical challenges of building X-RHex; and Boston Dynamics, Inc., which kindly provided comparison information regarding Rugged RHex.

G. C. Haynes is supported by an IC Postdoctoral Research Fellowship. This work was funded in part by the National Science Foundation under FIBR award 0425878 and in part by the Army Research Laboratory under Cooperative Agreement Number W911NF-10-2-0016. The views and conclusions contained in this document are those of the authors and should not be interpreted as representing the official policies, either expressed or implied, of the Army Research Laboratory or the U.S. Government. The U.S. Government is authorized to reproduce and distribute reprints for Government purposes notwithstanding any copyright notation herein.

References

[1] U. Saranlı, M. Buehler, and D. E. Koditschek, "RHex: A Simple and Highly Mobile Hexapod Robot," *The International Journal of Robotics Research*, vol. 20, no. 7, pp. 616–631, 2001.

[2] D. McMordie and M. Buehler, "Towards pronking with a hexapod robot," in *International Conference on Climbing and Walking Robots*, Karlsruhe, Germany, September 2001.

[3] H. Komsuoğlu, D. McMordie, U. Saranlı, N. Moore, M. Buehler, and D. Koditschek, "Proprioception based behavioral advances in a hexapod robot," in *Proceedings of the IEEE International Conference on Robotics and Automation*, 2001.

[4] U. Saranlı, A. Rizzi, and D. Koditschek, "Model-based dynamic self-righting maneuvers for a hexapedal robot," *The International Journal of Robotics Research*, vol. 23, no. 9, p. 903, 2004.

[5] E. Z. Moore, D. Campbell, F. Grimminger, and M. Buehler, "Reliable stair climbing in the simple hexapod 'RHex'," in *Proceedings of the IEEE International Conference on Robotics and Automation*, vol. 3, 2002, pp. 2222–2227.

[6] N. Neville, M. Buehler, and I. Sharf, "A bipedal running robot with one actuator per leg," in *Proceedings of the IEEE International Conference on Robotics and Automation*, 2006.

[7] Boston Dynamics, Inc., "RHex Devours Rough Terrain." [Online]. Available: http://www.bostondynamics.com/robot_rhex.html

[8] C. Prahacs, A. Saunders, M. K. Smith, D. McMordie, and M. Buehler, "Towards legged amphibious mobile robotics," *Journal of Engineering Design and Innovation*, vol. 1P, 2005.

[9] Boston Dynamics, "RHex Datasheet," 2007.

[10] J. D. Weingarten, D. E. Koditschek, H. Komsuoğlu, and C. Massey, "Robotics as the delivery vehicle: A contextualized, social, self paced, engineering education for life-long learners," in *Robotics Science and Systems Workshop on "Research in Robots for Education"*, 2007.

[11] G. Dudek, P. Giguere, C. Prahacs, S. Saunderson, J. Sattar, L. Torres-Mendez, M. Jenkin, A. German, A. Hogue, A. Ripsman, *et al.*, "AQUA: An amphibious autonomous robot," *Computer*, vol. 40, no. 1, pp. 46–53, 2007.

[12] U. Saranlı, A. Avcı, and M. C. Öztürk, "A Modular, Real-Time Fieldbus Architecture for Mobile Robotic Platforms." *IEEE Transactions on Instrumentation and Measurement*, 2010, accepted.

[13] G. C. Haynes, A. Khripin, G. Lynch, J. Amory, A. Saunders, A. A. Rizzi, and D. E. Koditschek, "Rapid pole climbing with a quadrupedal robot," in *Proceedings of the IEEE International Conference on Robotics and Automation*, May 2009, pp. 2767–2772.

[14] E. Moore, "Leg design and stair climbing control for the RHex robotic hexapod," Master's thesis, McGill University, 2002.

[15] E. Shigley, *Mechanical Engineering Design*. McGraw-Hill, Inc., 1977.

[16] M. Ashby, *Materials selection in mechanical design*. Butterworth-Heinemann, 2005.

[17] C. Sommer, S. Sommer, and C. Sommer, *Wire EDM Handbook*. Advance Publishing, 2000.

[18] U. Kafader, *The Selection of High-Precision Microdrives*. Maxon Academy, 2006.

[19] D. Campbell and M. Buehler, "Preliminary bounding experiments in a dynamic hexapod," *Experimental Robotics VIII*, pp. 612–621, 2003.

[20] J. D. Weingarten, G. A. D. Lopes, M. Buehler, R. E. Groff, and D. E. Koditschek, "Automated gait adaptation for legged robots," in *Proceedings of the IEEE International Conference on Robotics and Automation*, vol. 3, 2004, pp. 2153–2158.

[21] A. De, G. Lynch, A. M. Johnson, and D. E. Koditschek, "Motor selection using task specifications and thermal limits," in *IEEE International Conference on Technologies for Robot Applications*, 2011, submitted.

[22] M. Mani, "A quick overview on rotatory Brush and Brushless DC Motors," Motion Control Department, Ingenia, Barcelona, Spain, Tech. Rep., 2006.

[23] I. Poulakakis, J. A. Smith, and M. Buehler, "Experimentally validated bounding models for the Scout II quadrupedal robot," in *ICRA*, 2004, pp. 2595–2600.

[24] D. DeWitt and F. Incropera, *Fundamentals of heat and mass transfer*. Wiley New York, 1996.

[25] Maxon Motors, "Maxon Catalog, Key Information," pp. 36–43, 2009–2010.

[26] ADVANCED Motion Controls , "DriveWare Software Manual," January 2009. [Online]. Available: http://www.a-m-c.com/download/manual/AMC_DriveWareSoftwareManual.pdf

[27] Wikipedia, "Rechargeable Batteries," June 2010. [Online]. Available: http://en.wikipedia.org/wiki/Rechargeable_battery

[28] J. Tarascon and M. Armand, "Issues and challenges facing rechargeable lithium batteries," *Nature*, vol. 414, no. 6861, pp. 359–367, 2001.

[29] C. F. Dalziel, "Electric shock hazard," *IEEE Spectrum*, vol. 9, no. 2, pp. 41–50, February 1972.

[30] Thunder Power RC, "Important Safety Instructions and Warnings," June 2010. [Online]. Available: http://thunderpowerrc.com/PDF/THPSafetyWarnings.pdf

[31] M. Quigley, B. Gerkey, K. Conley, J. Faust, T. Foote, J. Leibs, E. Berger, R. Wheeler, and A. Ng, "ROS: an open-source Robot Operating System."

[32] B. Gerkey, R. Vaughan, and A. Howard, "The Player/Stage project: Tools for multi-robot and distributed sensor systems," in *Proceedings of the 11th International Conference on Advanced Robotics*. Citeseer, 2003, pp. 317–323.

[33] United States. Dept. of Defense. Army Armament Research, Development and Engineering Center, *Dimensioning of Accessory Mounting Rail for Small Arms Weapons*, June 1999, MIL-STD-1913.

[34] H. Schempf, "Ultra-rugged soldier-robot for urban conflict missions," in *Unmanned Systems 2003 Conference - AUVSI 30th Annual Symposium and Exhibition*, July 2003.

[35] iRobot Corporation, "iRobot PackBot 510 with FasTac Kit," 2009. [Online]. Available: http://www.irobot.com/gi/filelibrary/pdfs/robots/iRobot_510_PackBot_for_Infantry_Troops.pdf

[36] L. Pan, L. Gu, and J. Xu, "Implementation of medical image segmentation in CUDA," in *International Conference on Information Technology and Applications in Biomedicine*, 2008, pp. 82–85.

[37] J. Kider, M. Henderson, M. Likhachev, and A. Safonova, "High-dimensional Planning on the GPU," in *Proceedings of the IEEE International Conference on Robotics and Automation*, 2010.

[38] NVIDIA, *NVIDIA CUDA Programming Guide 2.0*, 2008.

[39] D. Lowe, "Distinctive image features from scale-invariant keypoints," *International Journal of Computer Vision*, January 2004.

[40] C. Wu, "SiftGPU: A GPU implementation of scale invariant feature transform (SIFT)," http://cs.unc.edu/~ccwu/siftgpu, 2007.

[41] H. Bay, T. Tuytelaars, and L. Van Gool, "SURF: Speeded up robust features," in *Computer Vision - ECCV 2006*, ser. Lecture Notes in Computer Science, A. Leonardis, H. Bischof, and A. Pinz, Eds. Springer Berlin / Heidelberg, 2006, vol. 3951, pp. 404–417. [Online]. Available: http://dx.doi.org/10.1007/11744023_32

[42] N. Cornelis and L. Van Gool, "Fast scale invariant feature detection and matching on programmable graphics hardware," in *IEEE Computer Society Conference on Computer Vision and Pattern Recognition Workshops, 2008. CVPR Workshops 2008*, 2008, pp. 1–8.

[43] G. A. D. Lopes and D. E. Koditschek, "Visual registration and navigation using planar features," in *Proceedings of the IEEE Conference of Robotics and Automation*. IEEE, 2003.

[44] K. C. Galloway, "Passive variable compliance for dynamic legged robots," Ph.D. dissertation, Mechanical Engineering and Applied Mechanics, University of Pennsylvania, Philadelphia, PA, June 2010.

[45] P.-C. Lin, H. Komsuoğlu, and D. E. Koditschek, "Sensor data fusion for body state estimation in a hexapod robot with dynamical gaits," *IEEE Transactions on Robotics*, vol. 22, no. 5, pp. 932–943, October 2006.

[46] S. Skaff, A. Rizzi, and H. Choset, "Context identification for efficient multiple-model state estimation," in *Proceedings of the IEEE/RSJ International Conference on Intelligent Robots and Systems*, 2007, pp. 2435–2440.

[47] J. Weingarten, R. Groff, and D. Koditschek, "A framework for the coordination of legged robot gaits," in *Proceedings of the IEEE International Conference on Robotics and Automation*, 2004, pp. 679–686.

[48] G. C. Haynes and A. A. Rizzi, "Gaits and gait transitions for legged robots," in *Proceedings of the IEEE International Conference on Robotics and Automation*, Orlando, FL, USA, May 2006, pp. 1117–22.

[49] P. Giguere, G. Dudek, C. Prahacs, and S. Saunderson, "Environment identification for a running robot using inertial and actuator cues," in *Proceedings of Robotics Science and System (RSS)*, 2006.

[50] A. M. Johnson, G. C. Haynes, and D. E. Koditschek, "Disturbance Detection, Identification, and Recovery by Gait Transition in Legged Robots," in *Proceedings of the IEEE/RSJ Intl. Conference on Intelligent Robots and Systems*, 2010.

[51] R. Altendorfer, D. E. Koditschek, and P. Holmes, "Stability Analysis of Clock-driven Rigid-Body SLIP Model for RHex," *The International Journal of Robotics Research*, vol. 23, no. 10-11, pp. 1001–1012, 2004.

[52] T. Kubow and R. Full, "The role of the mechanical system in control: a hypothesis of self-stabilization in hexapedal runners," *Philosophical Transactions of the Royal Society of London Series B-Biological Sciences*, vol. 354, no. 1385, pp. 849–861, 1999.

[53] J. Chestnutt, M. Lau, G. Cheung, J. Kuffner, J. Hodgins, and T. Kanade, "Footstep planning for the Honda ASIMO humanoid," in *Proceedings of the IEEE International Conference on Robotics and Automation*. IEEE, 2006, pp. 629–634.

[54] P. Vernaza, M. Likhachev, S. Bhattacharya, S. Chitta, A. Kushleyev, and D. Lee, "Search-based planning for a legged robot over rough terrain," in *Proceedings of the IEEE International Conference on Robotics and Automation*. IEEE, 2009, pp. 2380–2387.

[55] J. Cham, S. Bailey, J. Clark, *et al.*, "Fast and robust: Hexapedal robots via shape deposition manufacturing," *The International Journal of Robotics Research*, vol. 21, no. 10-11, p. 869, 2002.

[56] L. Jackel, E. Krotkov, M. Perschbacher, J. Pippine, and C. Sullivan, "The DARPA LAGR program: Goals, challenges, methodology, and phase I results," *Journal of Field Robotics*, vol. 23, no. 11-12, pp. 945–973, 2006.

[57] "Special Issue on the DARPA Grand Challenge, Parts I & II," *Journal of Field Robotics*, vol. 23, no. 8-9, 2006.

[58] "Special Issue on the 2007 DARPA Urban Challenge, Parts I, II & III," *Journal of Field Robotics*, vol. 25, no. 8-10, 2008.

[59] G. A. Lynch, L. Rome, and D. E. Koditschek, "Sprawl angle in simplified models of vertical climbing: implications for robots and roaches," in *International Conference on Applied Bionics and Biomechanics*, Venice, Italy, 2010.

[60] J. Hollerbach, I. Hunter, and J. Ballantyne, "A comparative analysis of actuator technologies for robotics," in *The robotics review 2*. MIT Press, 1992, p. 342.

[61] R. Full, *Efficiency and Economy in Animal Physiology*. Cambridge University Press, 1991, ch. Concepts of efficiency and economy in land locomotion, pp. 97–131.

[62] R. Kornbluh, R. Pelrine, J. Eckerle, and J. Joseph, "Electrostrictive polymer artificial muscle actuators," in *Proceedings of the IEEE International Conference on Robotics and Automation*, 1998, pp. 2147–2154.